



## A physical interpretation of impedance at conducting polymer/electrolyte junctions

Eleni Stavrinidou, Michele Sessolo, Bjorn Winther-Jensen, Sébastien Sanaur, and George G. Malliaras

Citation: *AIP Advances* **4**, 017127 (2014); doi: 10.1063/1.4863297

View online: <http://dx.doi.org/10.1063/1.4863297>

View Table of Contents: <http://scitation.aip.org/content/aip/journal/adva/4/1?ver=pdfcov>

Published by the [AIP Publishing](#)

---

### Articles you may be interested in

[Effects of proton-conducting electrolyte microstructure on the performance of electrolyte-supported solid oxide fuel cells](#)

*J. Renewable Sustainable Energy* **5**, 021412 (2013); 10.1063/1.4798491

[Effect of Complexation of NaCl Salt with Polymer Blend \(PEO/PVP\) Electrolytes on Ionic Conductivity and Optical Energy Band Gaps](#)

*AIP Conf. Proc.* **1391**, 641 (2011); 10.1063/1.3643635

[Contribution of the electrode-electrolyte interface to the impedance of an electrolytic cell](#)

*J. Appl. Phys.* **104**, 114111 (2008); 10.1063/1.3033392

[Impedance spectroscopy analysis of an electrolytic cell limited by Ohmic electrodes: The case of ions with two different diffusion coefficients dispersed in an aqueous solution](#)

*J. Appl. Phys.* **102**, 104111 (2007); 10.1063/1.2809452

[Determination of the electronic conductivity of polybithiophene films at different doping levels using in situ electrochemical impedance measurements](#)

*Appl. Phys. Lett.* **83**, 2178 (2003); 10.1063/1.1609657

---

An advertisement for AIP's Journal of Computational Tools and Methods. It features a row of tablet devices displaying the journal's cover, which has a colorful, abstract pattern. The text 'computing' is written in a stylized font, with 'SCIENCE & ENGINEERING' underneath. Below the tablets, the text reads 'AIP'S JOURNAL OF COMPUTATIONAL TOOLS AND METHODS. AVAILABLE AT MOST LIBRARIES.'

**computing**  
SCIENCE & ENGINEERING

AIP'S JOURNAL OF COMPUTATIONAL TOOLS AND METHODS.  
**AVAILABLE AT MOST LIBRARIES.**

## A physical interpretation of impedance at conducting polymer/electrolyte junctions

Eleni Stavrinidou,<sup>1</sup> Michele Sessolo,<sup>1</sup> Bjorn Winther-Jensen,<sup>2</sup>  
Sébastien Sanaur,<sup>1</sup> and George G. Malliaras<sup>1,a</sup>

<sup>1</sup>Department of Bioelectronics, Ecole Nationale Supérieure des Mines, CMP-EMSE,  
MOC 880 route de Mimet, 13541 Gardanne, France

<sup>2</sup>Department of Materials Engineering, Monash University, Clayton, VIC 3800, Australia

(Received 10 November 2013; accepted 12 January 2014; published online 23 January 2014)

We monitor the process of dedoping in a planar junction between an electrolyte and a conducting polymer using electrochemical impedance spectroscopy performed during moving front measurements. The impedance spectra are consistent with an equivalent circuit of a time varying resistor in parallel with a capacitor. We show that the resistor corresponds to ion transport in the dedoped region of the film, and can be quantitatively described using ion density and drift mobility obtained from the moving front measurements. The capacitor, on the other hand, does not depend on time and is associated with charge separation at the moving front. This work offers a physical description of the impedance of conducting polymer/electrolyte interfaces based on materials parameters. © 2014 Author(s). All article content, except where otherwise noted, is licensed under a Creative Commons Attribution 3.0 Unported License. [<http://dx.doi.org/10.1063/1.4863297>]

Conjugated polymers represent an important class of organic electronic materials partly because of their ability to conduct both electronic and ionic carriers.<sup>1,2</sup> A variety of (opto-)electronic devices rely on this key property of mixed conductivity for their operation.<sup>3-9</sup> Of particular contemporary interest is the electrically doped form of these materials (called conducting polymers). These materials are finding a host of applications in bioelectronics, as transducers and actuators of biological phenomena.<sup>9-13</sup> A widely used conducting polymer is PEDOT:PSS, in which the semiconducting poly(3,4-ethylenedioxythiophene) (PEDOT) is heavily doped *p*-type by the sulfonate anions (acceptors) of the poly(styrene sulfonate) (PSS).<sup>14</sup> Although our understanding of electronic transport in conjugated polymers has reached a high level of sophistication,<sup>15,16</sup> ion transport has not received the same amount of attention, mainly due to the lack of suitable characterization techniques. While conductivity or diffusion measurements can be used to study ion transport in materials that conduct only ions (such as polymer electrolytes),<sup>17</sup> these techniques are difficult to apply in mixed conductors because the simultaneous presence of electronic carriers greatly complicates data analysis. There is a need, therefore, for new experimental approaches that provide insight on the fundamentals of ion transport in conjugated polymers.

Electrochemical impedance spectroscopy (EIS) is a common technique for studying charging and transport phenomena in conjugated polymers,<sup>18</sup> despite the fact that the interpretation of the obtained data can be model-dependent. In the most usual configuration, a thin polymer film is deposited on a metallic substrate (working electrode) and is placed in an electrochemical cell. A dc bias applied between the electrolyte and the electrode leads to ion injection from the electrolyte into the polymer and sets the doping level (redox state) of the latter. The injection of cations in PEDOT:PSS, for example, will decrease the hole density and dedope the film. Once the desired doping level is reached, a small ac modulation is applied and the impedance spectrum is recorded.

---

<sup>a</sup>Author to whom correspondence should be addressed. Electronic mail: [malliaras@emse.fr](mailto:malliaras@emse.fr).



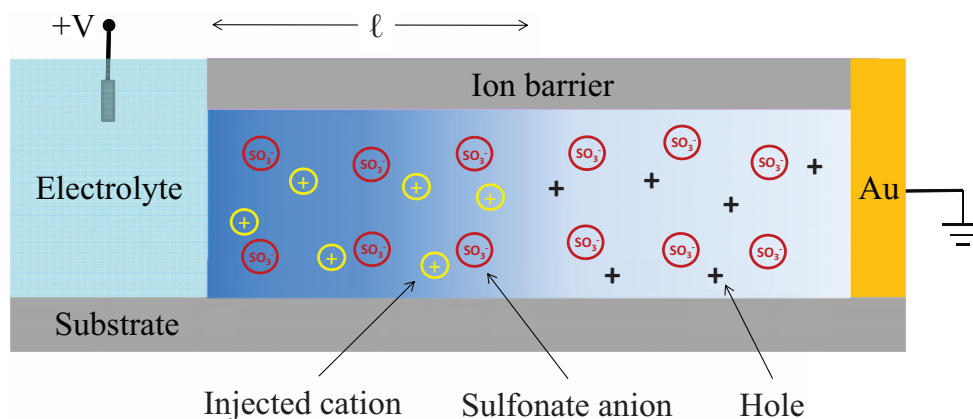


FIG. 1. Schematic representation of the device indicating the charge distribution in the film during the propagation of the dedoping front, at a distance  $\ell$  from the interface with the electrolyte.

Impedance is essentially the phase lag in the movement of charge carriers upon the application of the ac voltage. Since both ionic and electronic carriers move simultaneously, the analysis becomes complicated.<sup>19</sup> In the simplest case, an equivalent circuit consisting of several elements is used to fit the data, considering the path of an ion moving from the electrolyte to the bulk of the polymer. These elements include a resistor to describe transport in the electrolyte, a capacitor (usually modeled with a constant phase element) in parallel with a charge transfer resistor to model the process of ion injection into the film, and a diffusion element (modeled with a Warburg or a constant phase element) to capture ion diffusion inside the polymer.<sup>20</sup>

An alternative approach to study ion injection and transport in conjugated polymers is the so-called “moving front” experiment,<sup>21–23</sup> which relies on the fact that the optical absorption spectra of these materials change upon doping (electrochromism). In this experiment, changes in the optical density are spatially and temporally resolved in order to infer the injection and transport of ions inside a polymer film. A key difference between EIS and the moving front experiment is that in the former doping undergoes a small ac modulation around a fixed level, while in the latter there exist two regions in the film with distinctly different doping levels. We recently carried out a moving front experiment in a planar electrolyte/PEDOT:PSS/Au device, in which injected cations compensate the sulfonate acceptors and lead to hole depletion (the holes are extracted at the Au electrode). As a result, a dedoped region forms inside the PEDOT:PSS film that extends a distance  $\ell(t)$  from the interface with the electrolyte, where  $\ell(t)$  is the drift length of the injected cations at time  $t$ . The one-dimensional geometry of the planar junction allowed a straightforward visualization of ion drift inside the polymer, and enabled the extraction of the drift mobility of various cations.<sup>24</sup> Ion mobilities measured in PEDOT:PSS were found to be similar to values measured in water, consistent with transport in water channels inside a highly hydrated film.<sup>24</sup>

In this Letter we report on electrochemical impedance spectroscopy performed during a moving front experiment on a planar electrolyte/PEDOT:PSS junction. Impedance spectra acquired during the propagation of the dedoping front are modeled by an equivalent circuit of a resistor in parallel with a capacitor. We show that the resistor corresponds to ion transport in the dedoped region of the film, and can be quantitatively described using ion density and drift mobility, while the capacitor is associated with doping/dedoping processes at the moving front.

Figure 1 shows a schematic of the experimental configuration. A PEDOT:PSS film, deposited on a parylene-coated glass substrate, was coated with a layer of SU-8. The latter served as an ion barrier and prohibited ion injection into the PEDOT:PSS film from the top. Using photolithography, a well was created in the SU8/PEDOT:PSS stack and filled with an electrolyte, forming a planar electrolyte/PEDOT:PSS junction. The thickness of the PEDOT:PSS film was 400 nm, and its width was 26 mm. A polydimethylsiloxane rim was placed on top of the SU-8 well to confine 1.5–2 mL of electrolyte. A large area Pt counter electrode and a Ag/AgCl (3M KCl) reference electrode were

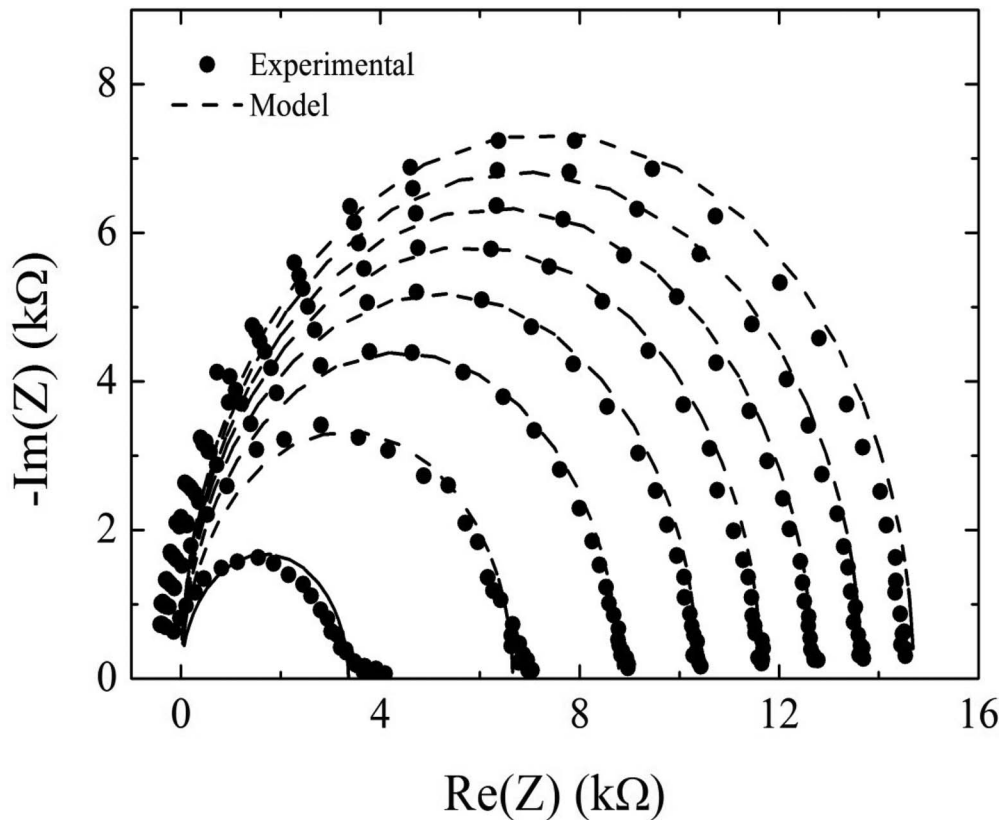


FIG. 2. Nyquist representation of eight impedance spectra (solid circles) recorded during a moving front experiment. The dashed lines are fits to an equivalent circuit model of a resistor in parallel with a capacitor.

immersed into the electrolyte (0.01 M KCl in deionized water), while a Au electrode, positioned at a distance  $L = 32 \text{ mm}$  from the electrolyte interface, provided electrical contact to the PEDOT:PSS film. The PEDOT:PSS/Au structure was connected with the potentiostat (Bio-Logic-Science Instruments) as the working electrode. The experiment was carried out as follows: Starting with the film in the  $p$ -doped state, a DC bias of 1 V was applied between the reference electrode and the Au contact, injecting  $\text{K}^+$  cations and beginning the dedoping of the PEDOT:PSS film. As the dedoping front propagates, we added an ac modulation with an amplitude of 100 mV and a frequency that was scanned from 100 kHz to 100 Hz in order to obtain the impedance spectra. The frequency range was limited by the need to minimize the duration of the EIS measurement: Each spectrum took approximately 5 s to acquire and there was a “dead” time of 12 s before a subsequent acquisition, during which time the dedoping front continued to progress inside the polymer film. A total of 8 spectra were acquired, well before the dedoping front reached the Au electrode. Consequently the applied voltage was set to zero and the film is allowed to return to its initial  $p$ -doped state. This defined one cycle; we performed a couple of cycles to a pristine device in order to allow the film to properly hydrate and the measurements to become reproducible. The data shown hereafter correspond to appropriate cycled films.

Impedance spectra are shown on the Nyquist plot of Fig. 2 as solid points. Each spectrum shows the typical semicircle behavior associated with an equivalent circuit of a resistor,  $R$ , in parallel with a capacitor,  $C$ . As time moves forward and the moving front propagates inside the film, the diameter of the semicircles increases. The right hand side (low frequency) end of a semicircle corresponds to the value of the resistor. It can be immediately seen that this value depends on time in a sub-linear fashion, as the distance between the low-frequency ends of successive semicircles decreases with each time scan. The value of the capacitor, on the other hand, is not as straightforward to appreciate from the Nyquist plots. In order to extract the exact time dependence of the resistor and

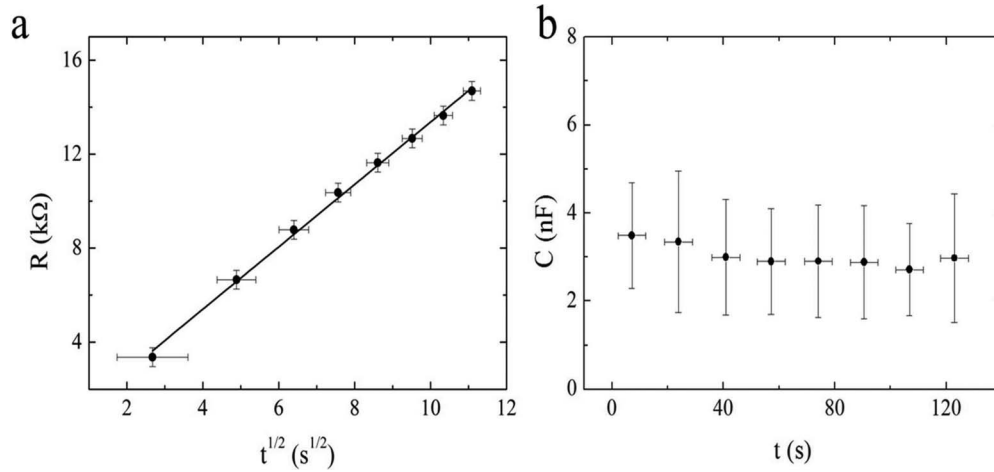


FIG. 3. Temporal evolution of the resistor (a) and the capacitor (b) determined from the impedance spectra. The line in (a) is a fit to Eq. (2).

the capacitor, a fit to an equivalent circuit consisting of  $R$  and  $C$  in parallel was performed for each spectrum (dashed lines in Fig. 2). The extracted values for  $R$  and  $C$  are shown in Fig. 3. Each data point in these plots is associated with the time corresponding to the end of the scan, as this condition reflects more accurately the point in time where the resistor is determined. The error bar on the x-axis reflects the duration of a scan. The error bars on the y-axis, on the other hand, were estimated from the high frequency end of the semicircles of Fig. 2, which show negative values for the real part of the impedance. This is due to an experimental artifact and these values were taken to represent the error in  $R$ , while the error in  $C$  was subsequently calculated from the fit.

The resistor in Fig. 3(a) is shown to increase with the square root of time, a trend that can be understood by means of the physical picture developed from the moving front experiment: Given that the dedoped region of the film is the least conducting element of the whole device, and given that its length grows with time, the resistor must be associated with this region. As a matter of fact, the length of the dedoped region grows as:<sup>25</sup>

$$l(t) = \sqrt{2 \cdot \mu \cdot V \cdot t}, \quad (1)$$

where  $\mu$  is the  $K^+$  drift mobility inside the PEDOT:PSS film and  $V$  is the applied dc voltage. Assuming that the  $K^+$  cations are the only mobile charges in the dedoped region, the corresponding resistance is equal to:

$$R(t) = \frac{\sqrt{2 \cdot V \cdot t}}{e \sqrt{\mu \cdot P \cdot A}}, \quad (2)$$

where  $P$  is the  $K^+$  density inside the PEDOT:PSS film,  $A$  is its cross section of the film, and  $e$  is the charge of an electron. The fact that the resistor in Fig. 3(a) follows the predicted  $R(t) \sim \sqrt{t}$  behavior supports the proposed physical interpretation. Namely, the resistive part of the impedance spectra is consistent with the temporal evolution of the moving front and is therefore associated with ion drift in the dedoped region of the film. The line in Fig. 3(a) is a fit to Eq. (2), yielding  $\sqrt{\mu \cdot P} = 6.6 \cdot 10^{19} \text{ V}^{-1} \text{ s}^{-1} \text{ cm}^{-1}$ . This value is within order of magnitude and only three times different of the one determined from the moving front experiment ( $\sqrt{\mu \cdot P} = 2.2 \cdot 10^{19} \text{ V}^{-1} \text{ s}^{-1} \text{ cm}^{-1}$ ), indicating that experimental values of ion density and mobility can be used to estimate the resistive part of the impedance. In fact, the agreement is even better if we account for the fact that the cross section  $A$  in Eq. (2) is underestimated, as PEDOT:PSS swells in contact with the electrolyte.<sup>24</sup>

Contrary to the resistor, the capacitor is shown in Fig. 3(b) to remain constant and equal to  $\sim 3 \text{ nF}$ . This suggests that the capacitor cannot be attributed to the dedoped region of the film, but rather to an interfacial capacitance. We attribute this capacitance to the leading front of the dedoped region, at which holes recede towards the Au electrode while  $K^+$  cations move in to take



their place. Given that holes in PEDOT:PSS are considerably more mobile than  $K^+$  cations,<sup>24</sup> a thin region develops right at the moving front interface in which holes are extracted but cations are not yet been injected. This region contains net negative charge due to uncompensated sulfonate acceptors. Considering the cations as slow moving compared to the holes, leads to a configuration that is analogous to charge redistribution near an electrode/electrolyte interface and hence leads to capacitance of the same magnitude as that of a double layer. Indeed, normalizing the experimental values for the cross section of the PEDOT:PSS film yields a capacitance per unit area of  $\sim 30 \mu F/cm^2$ , a value consistent with double layer capacitance.

The moving front experiment has shown that drift of ions is important for understanding electrochemical doping/dedoping in conjugated polymer films,<sup>25–28</sup> a fact that is often neglected in the interpretation of electrochemical impedance data. The latter describe ion transport in the film primarily as a result of diffusion, driven by the accumulation of ions at the electrolyte/polymer interface. According to this picture the applied potential drops partially at the electrolyte/polymer interface and determines in a self-consistent way the ion concentration at this interface. Ions then enter the film, driven by the concentration gradient between interface and bulk. In hydrated films that support high ion mobilities, however, ions enter the film with ease, leading to negligible potential drop at the electrolyte/polymer interface.<sup>25</sup> As a result, drift plays a significant role in bringing ions in the film and changing the doping level. In this work impedance spectra were determined solely on the basis of drift.

Electrochemical impedance is usually measured in thin films deposited on a metallic electrode. In such a configuration, given an ion mobility of  $10^{-3} cm^2 V^{-1}s^{-1}$  (consistent with small metal cations injected in a highly hydrated film), an ac modulation of 10 mV, and a film thickness of 100 nm, it can be shown that for frequencies below  $\sim 100 kHz$  the ions are able to reach the back contact within a half-cycle. This leads to accumulation of ionic charge at the interface with the back contact and complicates the field distribution inside the film. It also limits the amount of ionic charge that can be stored in the polymer film and may lead to a capacitance that depends on its thickness. Planar junctions in which the ions can travel for several mm before reaching the back contact avoid these complications, and represent therefore a better experimental geometry for studying ion transport phenomena.

Finally, it should be mentioned that in the analysis presented here we make two assumptions, namely that there is no barrier for ion injection at the electrolyte/PEDOT:PSS interface and no barrier for hole extraction at the PEDOT:PSS/Au interface. The former is justified by the high ion mobilities measured with the moving front measurements, while the latter by the fact that the film is highly doped near the Au contact. These assumptions might not hold in the case of non-doped conjugated polymer films which are usually hydrophobic and depleted of electronic charge. Still, the methodology of combining moving front measurements and electrochemical impedance spectroscopy in planar junctions represents a powerful experiment that can help understand the impact of such barriers on ion transport.

In this work we performed electrochemical impedance spectroscopy during a moving front experiment in a planar junction between an electrolyte and PEDOT:PSS. The impedance spectra were consistent with an equivalent circuit of a time varying resistor in parallel with a capacitor. The resistor was found to correspond to ion transport in the dedoped region of the film, and was in good agreement with values of ion density and drift mobility obtained from the moving front measurements. The capacitor, on the other hand, was found to be constant with time, implying that it is associated with charge separation at the moving front. The interpretation given here helps demystify electrochemical impedance by describing it in the language of solid-state physics, using parameters such as ion density and drift mobility.

## ACKNOWLEDGMENTS

M.S. was supported through a Marie Curie Fellowship. The authors acknowledge funding from MASK, a Marie Curie International Research Staff Exchange Scheme. B.W.J. acknowledges fellowship funding from The Australian Research Council. We would like to thank Germà

Garcia-Belmonte (Universitat Jaume I), Nicholas Melosh (Stanford University), and Yvan Bonnassieux (Ecole Polytechnique) for fruitful discussions.

- <sup>1</sup> J. M. Leger, *Adv. Mater.* **20** (4), 837–841 (2008).
- <sup>2</sup> J. Leger, M. Berggren, and S. A. Carter, *Iontronics : Ionic carriers in organic electronic materials and devices*. (CRC Press, Boca Raton, 2011).
- <sup>3</sup> Q. Pei, G. Yu, C. Zhang, Y. Yang, and A. J. Heeger, *Science* **269** (5227), 1086–1088 (1995).
- <sup>4</sup> J. C. deMello, N. Tessler, S. C. Graham, and R. H. Friend, *Physical Review B* **57** (20), 12951–12963 (1998).
- <sup>5</sup> D. A. Bernards, S. Flores-Torres, H. D. Abruna, and G. G. Malliaras, *Science* **313** (5792), 1416–1419 (2006).
- <sup>6</sup> R. J. Mortimer, A. L. Dyer, and J. R. Reynolds, *Displays* **27**(1), 2–18 (2006).
- <sup>7</sup> H. D. Abruna, Y. Kiya, and J. C. Henderson, *Physics Today* **61**(12), 43–47 (2008).
- <sup>8</sup> D. Khodagholy, J. Rivnay, M. Sessolo, M. Gurfinkel, P. Leleux, L. H. Jimison, E. Stavriniidou, T. Herve, S. Sanaur, R. M. Owens, and G. G. Malliaras, *Nat Commun* **4** (2013).
- <sup>9</sup> E. Smela, *MRS Bull.* **33**(3), 197–204 (2008).
- <sup>10</sup> J. Rivnay, R. M. Owens, and G. G. Malliaras, *Chemistry of Materials* (2013).
- <sup>11</sup> J. Isaksson, P. Kjall, D. Nilsson, N. D. Robinson, M. Berggren, and A. Richter-Dahlfors, *Nat. Mater.* **6**(9), 673–679 (2007).
- <sup>12</sup> P. Lin and F. Yan, *Adv. Mater.* **24**(1), 34–51 (2012).
- <sup>13</sup> D. Khodagholy, T. Doublet, P. Quilichini, M. Gurfinkel, P. Leleux, A. Ghestem, E. Ismailova, T. Hervé, S. Sanaur, C. Bernard, and G. G. Malliaras, *Nat Commun* **4**, 1575 (2013).
- <sup>14</sup> A. Elschner, S. Kirchmeyer, W. Lövenich, U. Merker, and K. Reuter, in *PEDOT, Principles and Applications of an Intrinsically Conductive Polymer* (CRC Press, 2010), pp. 113–166.
- <sup>15</sup> H. T. Nicolai, M. Kuik, G. A. H. Wetzelaer, B. de Boer, C. Campbell, C. Risko, J. L. Bredas, and P. W. M. Blom, *Nat. Mater.* **11**(10), 882–887 (2012).
- <sup>16</sup> A. J. Kronemeijer, E. H. Huisman, I. Katsouras, P. A. van Hal, T. C. T. Geuns, P. W. M. Blom, S. J. van der Molen, and D. M. de Leeuw, *Physical Review Letters* **105**(15) (2010).
- <sup>17</sup> B. Smitha, S. Sridhar, and A. A. Khan, *Journal of Membrane Science* **259** (1–2), 10–26 (2005).
- <sup>18</sup> J. O. M. Bockris, A. K. N. Reddy, and M. E. Gamboa-Aldeco, *Modern electrochemistry*, 2nd ed. (Plenum Press, New York, 1998).
- <sup>19</sup> M. A. Vorotyntsev, J. P. Badiali, and G. Inzelt, *Journal of Electroanalytical Chemistry* **472**(1), 7–19 (1999).
- <sup>20</sup> R. Hass, J. Garcia-Canadas, and G. Garcia-Belmonte, *Journal of Electroanalytical Chemistry* **577**(1), 99–105 (2005).
- <sup>21</sup> K. Aoki, T. Aramoto, and Y. Hoshino, *Journal of Electroanalytical Chemistry* **340**(1–2), 127–135 (1992).
- <sup>22</sup> T. Johansson, N.-K. Persson, and O. Inganäs, *Journal of the Electrochemical Society* **151**(4), E119–E124 (2004).
- <sup>23</sup> X. Wang and E. Smela, *The Journal of Physical Chemistry C* **113**(1), 369–381 (2008).
- <sup>24</sup> E. Stavriniidou, P. Leleux, H. Rajaona, D. Khodagholy, J. Rivnay, M. Lindau, S. Sanaur, and G. G. Malliaras, *Adv. Mater.* **25** (32), 4488–4493 (2013).
- <sup>25</sup> E. Stavriniidou, P. Leleux, H. Rajaona, M. Fiochi, S. Sanaur, and G. G. Malliaras, *J. Appl. Phys.* **113**(24) (2013).
- <sup>26</sup> J. C. Lacroix, K. Fraoua, and P. C. Lacaze, *Journal of Electroanalytical Chemistry* **444**(1), 83–93 (1998).
- <sup>27</sup> F. Miomandre, M. N. Bussac, E. Vieil, and L. Zuppiroli, *Chemical Physics* **255**(2–3), 291–300 (2000).
- <sup>28</sup> X. Wang, B. Shapiro, and E. Smela, *The Journal of Physical Chemistry C* **113**(1), 382–401 (2008).